

## A Study of Defects in Iron Based Alloys by Positron Annihilation Techniques

K.M. MOSTAFA<sup>a,b,\*</sup>, J. DE BAERDEMAEKER<sup>a</sup>, P.R. CALVILLO<sup>b</sup>,  
N. VAN CAENEGEM<sup>b</sup>, Y. HOUBAERT<sup>b</sup> AND D. SEGERS<sup>a</sup>

<sup>a</sup>Department of Subatomic and Radiation Physics, Ghent University  
Proeftuinstraat 86, 9000 Ghent, Belgium

<sup>b</sup>Department of Metallurgy and Materials Sci., Ghent University  
Technologiepark 903, 9052 Ghent, Belgium

Defects in different iron based alloys were studied at room temperature using positron annihilation techniques. In FeSi alloys, it was found that the Si content and the deformation temperature affect the positron annihilation parameters. In Fe–Mn–Si–Cr–Ni–C samples with different deformations, positron lifetime measurements were carried out before and after isochronal annealing. X-ray diffraction gave information about the different microstructural phases that exist in the deformed alloys before and after annealing. During deformation a martensitic  $\epsilon$  phase is induced. At 500°C, defects and the  $\epsilon$  martensite phase were almost annealed out from the low deformed samples.

PACS numbers: 78.70.Bj, 62.20.F–

### 1. Introduction

The positron is a very sensitive probe, which can be used in detecting vacancy-type defects in metals [1–3]. Since positively charged nuclei are absent at vacancy-type defects, positrons are trapped and annihilate there with the surrounding electrons, conveying the information on the local electronic environment around the vacancy-type defects, therefore the defect structure after deformation of metallic samples can be investigated with the positron annihilation technique [4].

In the present work, the different types of defects are investigated which can be formed in FeSi as a result of the deformation temperature and the Si content. Alloying iron with silicon improves its magnetic performance by reducing the effect of magnetostriction, noise and energy losses, while the electrical resistivity increases.

---

\*corresponding author; e-mail: khaled.mostafa@UGent.be

Fe–Mn–Si–Cr–Ni–C is one of the promising shape memory alloys. The shape memory effect in FeMnSi alloys was first reported by Sato et al. [5]. The shape memory alloys (SMAs) are metallic materials, which have the ability to return to some previously defined shape when subjected to the appropriate thermal procedure. These materials can be plastically deformed at some relatively low temperature, and upon exposure to some higher temperature will return to their shape prior to the deformation. Materials that exhibit shape memory only upon heating are one-way shape memory alloys [6]. The FeMnSi-based shape memory alloys have attracted much attention in the recent time because of their low cost and excellent workability. The additions of Cr and Ni improve their shape memory effect (SME) and corrosion resistance [7, 8]. Their SME arises from the reverse transformation of stress-induced  $\varepsilon$  martensite (hcp structure) into  $\gamma$  austenite (fcc structure) upon heating by the movement of the Shockley partial dislocations.

## 2. Experimental

The chemical composition of the experimental FeSi alloys is shown in Table I. The production of the alloys is described in a previous publication [9]. Deformations were carried out by plane strain compression tests using a MTS machine with a maximum force capacity of 2500 kN. From the deformed and as-received material, samples with an area of 1 cm<sup>2</sup> perpendicular to the normal direction (ND) of deformation were prepared for positron annihilation measurements by mechanical polishing.

TABLE I

The chemical composition of the FeSi alloy.

Element [wt.%]	C	Si	Al	Mn	P	S	Ti	N
Steel A	0.002	1.88	0.075	0.048	0.016	0.009	0.002	0.03
Steel B	0.004	3.02	0.098	0.046	0.015	0.009	0.003	0.002
Steel C	0.003	4.06	0.096	0.066	0.016	0.009	0.003	0.007

TABLE II

The chemical composition of the Fe–Mn–Si–Cr–Ni–C alloy.

	Fe	Mn	Si	Cr	Ni	C
wt.%	66.84	12.56	6.09	9.44	4.89	0.18

The chemical composition of the Fe–Mn–Si–Cr–Ni–C alloy is given in Table II. These samples were cast in an air furnace, air cooled, reheated to 1200°C and hot rolled on a laboratory mill from 20 mm to 2 mm and air cooled. In

order to austenitize the samples, they were heated to 1100°C for 15 min and water quenched to room temperature. After deformation the specimens were cut, mechanically polished and then electrolytically polished in a solution of 20% perchloric acid and 80% butylcellosolve.

Positron lifetime measurements were performed at room temperature using a fast-fast lifetime spectrometer with 205 ps resolution. A positron source  $^{22}\text{NaCl}$  of about 10  $\mu\text{Ci}$  was sealed between two kapton foils with a thickness of 7.5  $\mu\text{m}$ . Each spectrum contained at least  $10^6$  counts and was analyzed with the program LT by Kansy [10]. The samples were measured at room temperature, and subsequently isochronally annealed for 15 min from 100 up to 500°C.

### 3. Results and discussion

#### 3.1. Positron annihilation lifetime

The calculated and measured positron lifetimes for different types of defects in pure iron and other iron based alloys are summarized in Table III.

TABLE III

The calculated and measured positron lifetimes for different types of defects in pure iron and other iron based alloys.

Material	Positron lifetime [ps]	Reference	Measured in Gent [ps]
Fe-bulk	110	[11]	107
Fe-dislocations	165	[12]	150–165
Fe-mono-vacancy	175	[11]	170–180
Fe-di-vacancy	197	[12]	
Fe-3 vacancy cluster	232	[12]	
Fe-4 vacancy cluster	262	[12]	
Fe-6 vacancy cluster	304	[12]	
FeSi (2,3 and 4 wt.% Si well annealed)			$108 \pm 3$
Fe <sub>75</sub> Si <sub>25</sub>	109	[13]	
Fe–Mn–Si–Cr–Ni(C)			$107 \pm 3$

We have measured the value for defect free Fe, Fe–MnS–Cr–Ni and FeSi. The values of the defect free lifetimes for those materials varied between 107–110 ps.

##### 3.1.1. FeSi

Three FeSi alloys with different Si content were studied. One set of samples was deformed at room temperature and another set of samples was deformed at high temperature (1000°C).

*Room temperature deformed samples.* Figure 1 shows the effect of deformation at room temperature on the positron annihilation lifetime and its intensities

for the alloys with different Si content. The trapping of the positrons in the defects is saturated. The two main annihilation sites for the positrons are dislocations with lifetime  $\tau_1 \approx 150$  ps and  $I_1 > 70\%$ , and small vacancy clusters (200–250 ps) or at higher content of Si (4 wt.%), bigger vacancy clusters (320 ps). Because of the saturation trapping of positrons in defect sites, the concentration of defects cannot be calculated directly from the data of lifetime only.

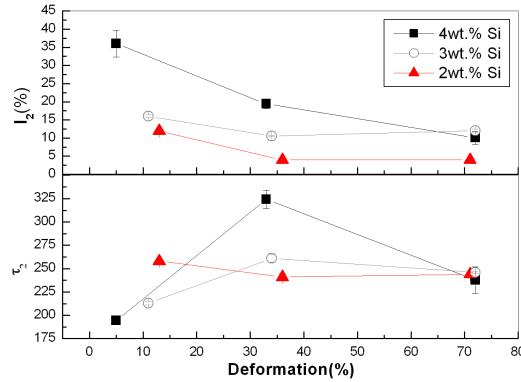


Fig. 1. The relation between positron annihilation lifetime  $\tau_2$  and its intensity ( $I_2$ ) for FeSi alloys of different contents of Si with different degrees of deformations (the shorter positron lifetime  $\tau_1$  is fixed to be 150 ps and its intensity is  $I_1 = 100 - I_2$ ).

*High temperature deformation.* Vacancy formation is a result of the thermodynamic demand of creating more entropy at elevated temperature in order to lower the overall free energy of the system. In case of pure metals and their disordered alloys, the formation of vacancies is the solution to create more (configurational) entropy. For intermetallics (i.e., ordered alloys), there are two ways of entropy production: one is to increase disorder by introducing “wrong” atoms (or antisite defect (ASD)) through atom exchange between different sublattices; the other is to introduce vacancies. Vacancies can affect the electrical, optical, and mechanical properties of the materials.

The positron annihilation lifetime value for the three undeformed FeSi alloys is  $108 \pm 3$  ps. For the 75% deformed alloys at high temperature (1000°C), there are two lifetime components.

Figure 2 shows the relation between the positron annihilation lifetime and the Si content. The value of the second component of the lifetime is around 185 ps. This value is related to existence of monovacancies [12, 14]. The other component, which is less than 100 ps, is the result of the annihilation of positrons in the defect free lattice. This reduced lifetime is a result of the trapping.

A quantitative analysis of the trapping rates and the vacancy concentration can be calculated using the two-state trapping model. Using the measured values for the positron annihilation lifetimes ( $\tau_1, \tau_2$ ) and their intensities ( $I_1, I_2$ ), the

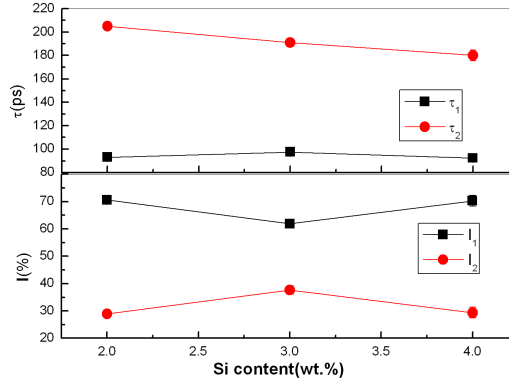


Fig. 2. The relation between the positron annihilation lifetime and the Si content.

mean lifetime of positrons annihilation lifetimes can be calculated using the following relation:

$$\tau_m = \tau_1 I_1 + \tau_2 I_2. \tag{1}$$

The positron trapping rate for vacancy  $\kappa_v$  can be calculated as

$$\kappa_v = \mu_v C_v = (\tau_m - \tau_b) / \tau_b (\tau_v - \tau_m), \tag{2}$$

$$\tau_b = (I_1 / \tau_1 + I_2 / \tau_2)^{-1}, \tag{3}$$

where  $\mu_v$  is the trapping coefficient for defects (vacancy),  $C_v$  is the vacancy concentration,  $\tau_b$  and  $\tau_v$  are the positron annihilation lifetime in bulk and in vacancy, respectively. The concentration of vacancies is calculated from Eq. (2) by giving the value of the trapping coefficient for a single vacancy in pure Fe,  $\mu_v = 1.1 \times 10^{15} \text{ s}^{-1}$  [12, 15].

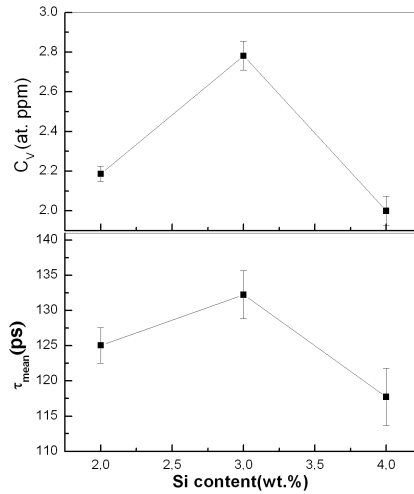


Fig. 3. The change of mean lifetime of positrons and vacancy concentration with the Si content.

Figure 3 shows the relation between the mean lifetime for positrons ( $\tau_m$ ) and the vacancy concentration  $C_v$  with the Si content. It was found that at 3 wt.% Si there is a maximum value for  $\tau_m$  and the vacancy concentration.

### 3.1.2. Fe–Mn–Si–Cr–Ni–C

Using the positron annihilation techniques, the effect of isochronal annealing on the deformation-induced defects and phase transition in Fe–Mn–Si–Cr–Ni–C is studied. A set of deformed Fe–Mn–Si–Cr–Ni–C samples (2–20% deformation) was annealed isochronally (15 min) starting from room temperature up to 500°C in steps of 100°C. The positron-lifetime spectra were fitted using two components. The trapping component has a positron lifetime around 150 ps. This value is shorter than that of the vacancies, which is 180 ps [16]. This value is attributed to positron annihilation in dislocations [17].

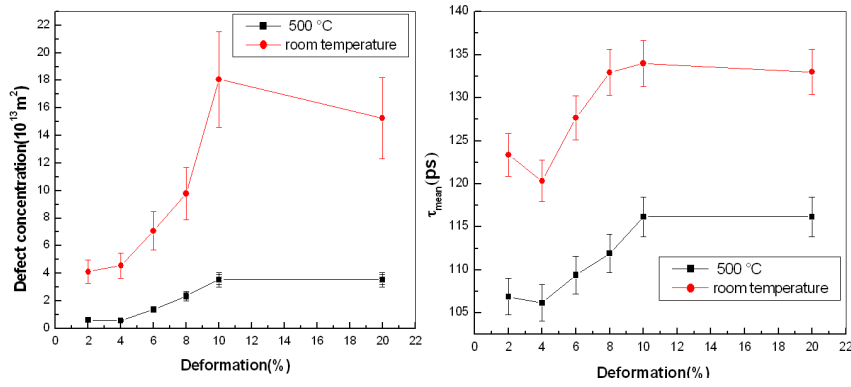


Fig. 4. The effect of annealing on the defect concentration and mean positron lifetime.

The temperature dependence of the mean value of the positron annihilation lifetime  $\tau_{\text{mean}}$  is shown in Fig. 4. The increase in deformation leads to an increase in the dislocation concentration and the  $\tau_{\text{mean}}$ . At 500°C, a significant decrease in  $\tau_{\text{mean}}$  is observed. For the low deformed samples (2, 4%) annealed at 500°C, most of the positrons annihilated in the defect free lattice, giving a lifetime near to 107 ps, which is close to the bulk value measured for these kind of alloys. This value is around 108 ps, which is the same value for the defect free samples. This means that the low deformed samples have almost no defects at 500°C. For the samples of deformation higher than 4%, the  $\tau_{\text{mean}}$  is higher than 108 ps. This means that these samples still have defects at the annealing temperature 500°C.

### 3.2. XRD

Figure 5a, b shows the X-ray diffraction (XRD) data for the 4% and 10% Fe–Mn–Si–Cr–Ni–C deformed samples at room temperature, and after the isochronal annealing at 500°C. The 4% deformed sample has almost no  $\epsilon$  phase at 500°C (Fig. 5b). If the deformation is small, the reverse movement of the Shockley

partials is not impeded because only primary  $\varepsilon$  variants moved through the parent austenite under the influence of stress. The microstructure of the 10% deformation still contains  $\varepsilon$  martensite. When the strain is large, several  $\varepsilon$  variants will be activated and the intersection of  $\varepsilon$  plates will impede the back movement of the partials. In addition, the plastic deformation of the austenite will be initiated at higher strains, such as 10%. The presence of dislocations in the parent phase prevents the free motion of the interface. This influence of the amount of pre-strain was also described before in [18–20].

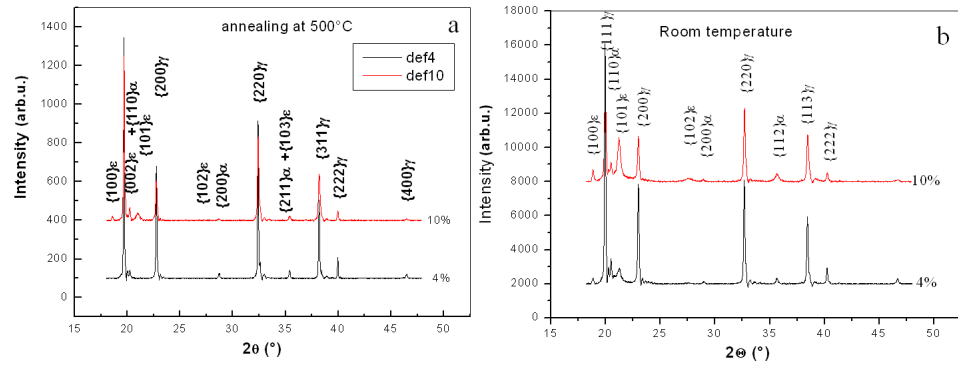


Fig. 5. XRD spectra for 4% and 10% deformation: (a) annealed at 500°C, (b) at room temperature.

The intensity of the  $(002)_\varepsilon$ ,  $(100)_\varepsilon$  peaks is higher for the 10% deformation compared to the one of the 4% deformation.

## 4. Conclusion

### 4.1. FeSi alloys

From the comparison of defects induced by deformation at room temperature and high temperature, it can be concluded that the type of defect depends on the deformation temperature. For the alloys deformed at high temperature the main defect is vacancy related. In case of the room temperature deformed alloys, it was found that the dislocation is the major defect, beside a small percentage related to the existence of vacancy clusters. Increasing the Si content increases the intensity of positrons trapped in vacancy clusters in the deformed alloys at room temperature.

### 4.2. Fe-Mn-Si-Cr-Ni-C

The increase in deformation leads to an increase in the dislocation concentration and the  $\tau_{\text{mean}}$ . At 500°C, a significant decrease in  $\tau_{\text{mean}}$  is observed. At 500°C the low deformed samples have almost no defects, while samples with a deformation more than 4% still have defects. The XRD shows that the intensity of the  $(002)_\varepsilon$ ,  $(100)_\varepsilon$  peaks is higher for the 10% deformation compared to the one

of the 4% deformation. The 4% deformed sample has almost no  $\varepsilon$  phase after the annealing at 500°C. The 10% deformed sample still has  $\varepsilon$  martensite phase.

### References

- [1] *Positron in Solids*, Ed. P. Hautojarvi, Springer-Verlag, Berlin 1979.
- [2] *Positron Solid-State Physics*, Eds. W. Brandt, A. Dupasquier North-Holland, Amsterdam 1983.
- [3] M.J. Puska, R.M. Nieminen, *Rev. Mod. Phys.* **66**, 841 (1994).
- [4] R. Krause-Rehberg, H.S. Leipner, *Positron Annihilation in Semiconductors*, Springer, Berlin 1999.
- [5] A. Sato, E. Chishima, K. Soma, T. Mori, *Acta Metall.* **30**, 1177 (1982).
- [6] H.C. Lin, K.M. Lin, Y.S. Chen, *J. Sur. Coatings Technol.* **194**, 68 (2005).
- [7] X.X. Wang, L.C. Zhao, *Scr. Metall. Mater.* **26**, 1451 (1992).
- [8] H. Otsuka, H. Yamada, H. Tanahashi, T. Maruyama, *Mater. Sci. Forum* **56**, 655 (1990).
- [9] P.R. Calvillo, Y. Houbaert, *Mater. Sci. Forum* **553**, 15 (2007).
- [10] J. Kansy, *Nucl. Instrum. Methods Phys. Res.* **374**, 235 (1996).
- [11] P. Hautojarvi, L. Pollanen, A. Vehanen, J. Yli-Kaupilla, *J. Nucl. Mater.* **114**, 250 (1983).
- [12] A. Vehanen, P. Hautojarvi, J. Johansson, J. Yli-Kaupilla, P. Moser, *Phys. Rev. B* **25**, 762 (1982).
- [13] E.A. Kummerle, K. Badura, B. Sepiol, H. Mehrer, H.E. Schaefer, *Phys. Rev. B* **52**, 6947 (1995).
- [14] M.J. Puska, R.M. Nieminen, *J. Phys. F, Met. Phys.* **13**, 333 (1983).
- [15] Y.-K. Park, J.T. Waber, M. Meshii, C.L. Snead, Jr., C.G. Park, *Phys. Rev. B* **34**, 823 (1986).
- [16] G. Kuamoto, Y. Asano, M. Takanaka, K. Kitajimi, *J. Phys. Soc. Jpn.* **53**, 1098 (1983).
- [17] C. Hidalgo, S. Linderoth, N. de Diego, *Philos. Mag. A* **64**, L61 (1986).
- [18] T. Shiming, Y. Shiwei, *Scr. Metall. Mater.* **27**, 229 (1992).
- [19] H. Inahaki, *Z. Metallkd.* **83**, 90 (1992).
- [20] N. Van Caenegem, L. Duprez, K. Verbeken, B.C. De Cooman, Y. Houbaert, D. Segers, *ISIJ Int. (Iron Steel Inst. Japan Int.)* **47**, 723 (2007).